

## Natural radioactivity of thermal springs and related precipitates in Gellért Hill area, Buda Thermal Karst, Hungary



Petra Kovács-Bodor<sup>a,e,\*</sup>, Katalin Csondor<sup>a</sup>, Anita Erőss<sup>a</sup>, Dénes Szieberth<sup>b</sup>, Ágnes Freiler-Nagy<sup>c</sup>, Ákos Horváth<sup>d</sup>, Árpád Bihari<sup>e</sup>, Judit Mádl-Szőnyi<sup>a,e</sup>

<sup>a</sup> József and Erzsébet Tóth Endowed Hydrogeology Chair, Department of Physical and Applied Geology, ELTE Eötvös Loránd University, Pázmány Péter Szny. 1/c, 1117, Budapest, Hungary

<sup>b</sup> Department of Inorganic and Analytical Chemistry, Budapest University of Technology and Economics, Műgyetem Rakpart 3, 1111, Budapest, Hungary

<sup>c</sup> Cemkut Kft., Bécsi út 122-124, 1034, Budapest, Hungary

<sup>d</sup> Department of Atomic Physics, ELTE Eötvös Loránd University, Pázmány Péter Szny. 1/a, 1117, Budapest, Hungary

<sup>e</sup> Isotope Climatology and Environmental Research Centre, Institute for Nuclear Research, Hungarian Academy of Sciences, Bem Tér 18/c, 4026, Debrecen, Hungary

### ABSTRACT

The elevated radioactivity of the thermal waters of Buda Thermal Karst (BTK), Hungary is known and studied since the beginning of the 20th century. In the recent studies, the anomalous  $^{222}\text{Rn}/^{226}\text{Ra}$  ratios have drawn the attention to the existence of local  $^{222}\text{Rn}$  source. Biogeochemical precipitates (i.e. biofilms) in spring caves were found to have high adsorption capacity, accumulating e.g.  $^{226}\text{Ra}$ . Biogeochemical precipitates are ubiquitous in the thermal springs of BTK, occurring in different amount and colours (dark grey, brown, red, white), and have different microbial communities and elemental composition. The detailed investigation of the radioactivity of spring waters highlighted the different  $^{226}\text{Ra}$  and  $^{222}\text{Rn}$  activity concentrations. The present study aimed to survey the radioactivity of the thermal springs of Gellért Hill area, together with the biogeochemical precipitates and air above the water level, and to assess the evolution of the radioactivity of known-aged precipitates, formed during in situ experiments. We found that the basic physicochemical parameters of the spring waters (field parameters, major ions) do not affect the adsorption capacity of biogeochemical precipitates. It was revealed by the conducted in situ experiments, that the flow conditions influence the evolution rate of precipitates, so their adsorption capacity. The  $^{222}\text{Rn}$  activity concentrations of spring waters are dependent on the area of the water surface, volume of air space above the water level, ventilation of the caves/channels and presence of calcite layer on the water surface. The latter has a blocking effect on degassing.

### 1. Introduction and goals

The elevated radioactivity of the thermal waters of Budapest, especially Gellért Hill area, is known since the beginning of the 20th century (Weszelszky, 1912). Before 2010, the radioactivity measurements focused mainly on the  $^{222}\text{Rn}$  and  $^{226}\text{Ra}$  activity of the waters (e.g. Alföldi et al., 1968; Baradács et al., 2001, 2002; Kasztovszky et al., 1996; summarized by Palotai et al., 2005). They reported anomalously high  $^{222}\text{Rn}$  activity concentrations (ACs) (up to 600  $\text{BqL}^{-1}$ ) compared to measured  $^{226}\text{Ra}$  ACs (up to 1000  $\text{mBqL}^{-1}$ ) in several spring and well waters of Budapest, especially around Rudas Spa, at the foothill of Gellért Hill. They also tried to identify the source of the elevated  $^{222}\text{Rn}$  content of the waters. Palotai et al. (2005) assumed three possible sources: faults, as the area is highly tectonized and faults are good transport routes for gases; lamprophyre dikes because of their magmatic origin; or both faults and dikes.

Later, a detailed measuring campaign was conducted in the springs and wells of Buda Thermal Karst which aimed the characterization of lukewarm and thermal waters and their mixing processes.  $^{226}\text{Ra}$  and

$^{222}\text{Rn}$  measurements were completed by  $^{234} + ^{238}\text{U}$  AC analysis, as these radionuclides can be used for the characterization of different waters due to their distinct geochemical behaviour (e.g. Eisenlohr and Surbeck, 1995; Hoehn, 1998). Based on this detailed study,  $^{226}\text{Ra}$  AC varied between 221 and 870  $\text{mBqL}^{-1}$ ,  $^{222}\text{Rn}$  between 3 and 963  $\text{BqL}^{-1}$  and  $^{234} + ^{238}\text{U}$  between 11 and 29  $\text{mBqL}^{-1}$  in the thermal waters (33–47 °C) of the Southern System (Gellért Hill area) of the Buda Thermal Karst (Erőss, 2010; Erőss et al., 2012). There was no linear connection between the AC of radionuclides and temperature or total dissolved solid content. Deep waters contained low ACs of  $^{222}\text{Rn}$ , suggesting a source close to the surface (Erőss et al., 2012). To identify the source of  $^{222}\text{Rn}$ , gamma-spectrometry measurements have been performed on different formations in Török Spring, one of the thermal springs in Gellért Hill area. It was found that red iron-hydroxide precipitates accumulate  $^{226}\text{Ra}$  in high concentrations (up to 1830  $\text{Bqkg}^{-1}$ ), causing high  $^{222}\text{Rn}$  activity of the spring water (621  $\text{BqL}^{-1}$ ). These precipitates were identified as biofilms (Borsodi et al., 2012), later called biogeochemical precipitates (Dobosy et al., 2016) because of their low TOC and high mineral content. Throughout this paper,

\* Corresponding author. Pázmány Péter sny. 1/c, 1117, Budapest, Hungary.  
E-mail address: [petrabodor@caesar.elte.hu](mailto:petrabodor@caesar.elte.hu) (P. Kovács-Bodor).

biogeochemical precipitates will be referred as BGP. Bacteria, inhabiting these BGPs are adapted to the radioactive environment (Makk et al., 2016; Enyedi et al., accepted).

Different coloured (white, brown, red, reddish brown, grey, black) BGPs and carbonate precipitates are known also from other springs of Buda Thermal Karst with distinct trace element content. Fe and Mn are the main elements responsible for brown, red etc. colours (Dobosy et al., 2016). The radionuclide content of the precipitates was not published yet, the only exception is the formations of Török Spring (Eröss, 2010; Eröss et al., 2012). A challenging question is the so called “age” of BGPs in the spring caves, which is difficult to tell, as their formation and precipitation rate have not been studied yet. Due to their newly recognized significance, their adsorbing capacity and the influencing factors of adsorption and different radioactivity of spring waters are also unknown in Buda Thermal Karst. Thus, the goals of the recent study were (1) to survey the radioactivity of different spring waters and related precipitates in the Gellért Hill area; (2) to better understand the connection between radioactivity and the physicochemical characteristics (flow conditions, field parameters, major ions) of the waters; (3) to assess the evolution of radioactivity of known-aged BGPs formed during in situ experiments.

## 2. Study area

Gellért Hill area is the Southern discharge zone of Buda Thermal Karst, in the capital city of Hungary, Budapest (Fig. 1), where thermal springs (33–47 °C) discharge (e.g. Alföldi et al., 1968; Erhardt et al., 2017; Eröss et al., 2012; Mádl-Szőnyi et al., 2017). As these thermal springs represent the terminal points of regional groundwater flow systems, the temporal changes of physicochemical parameters are low, mainly influenced by the water level of River Danube (Páll-Somogyi, 2010). Three spas were built to use the thermal waters of the area, Rác, Rudas and Gellért Spa (Fig. 2). Many spring caves were found during the construction of roads and spas. Nowadays, these springs are not used by the spas, they use shallow wells for production. Due to the urbanization of the area, the environment of most springs is built-in. So, their natural flow conditions have been changed and can no longer prevail, making the water movement quasi-stagnant, that it is immeasurable.

In this study, water and precipitates of four springs of the Gellért Hill area were studied: Rác Nagy, Rudas Török, Rudas Diana Hygieia Springs and Gellért Ósforrás (Fig. 3). The other springs cannot be

sampled because they are closed, or they have dried out. Furthermore, two in situ experiments were conducted, one in Rudas Török Spring and the other in Gellért Tunnel (Fig. 2.).

The spas and their springs are indicated by brown (Gellért Spa), blue (Rudas Spa) and orange (Rác Spa) throughout the paper on figures and in tables.

### 2.1. Rác Nagy Spring

Nagy Spring is located at the basement of Rác Spa (Fig. 2). There is a natural enlarged fissure (Fig. 4a) which was covered during the constructions of the spa. This covering part is concrete, the bottom parts are in the host rock (Fig. 3a).

### 2.2. Rudas Török Spring

Török Spring can be found at the foothill of Gellért Hill (Fig. 2). The spring pool can be found in a few m<sup>3</sup> volume spring cave (Fig. 4b). The cave was enlarged artificially, and a concrete floor was made above the water surface (Fig. 3b). The Török Spring as part of the springs of Rudas Spa were connected with a drain system (Fig. 2), which leads their water toward River Danube. The pool of Török Spring has an overflow toward this drain system. The original spring discharge is at the edge of the spring pool (Fig. 3b), but due to water production in the surroundings, the water level has been lowered and the water movement cannot be measured with conventional methods in the pool. Measurable water movement exists only at the overflow. This part can be reached through a manhole (Fig. 3b). The water is about 1 m deep in the pool and ~10 cm deep in the overflow.

### 2.3. Rudas Diana Hygieia Spring

Two springs were found during the construction of Rudas Spa, Diana and Hygieia Springs. Nowadays, they are under the basement of the spa, and have three branches which connect the formerly separated springs. Two of the three branches have natural spring discharges (Fig. 3c). The bottom parts of the branches are in dolomite, the host rock of Gellért Hill, while the upper part is in concrete (Fig. 4c). The spring group can be reached through a manhole from the basement of Rudas Spa (Fig. 3c). The water is about 1–2 m deep in the branches, depending on the water level of River Danube. Several mm-thick, continuous calcite raft is forming on the water surface (Fig. 4c), which

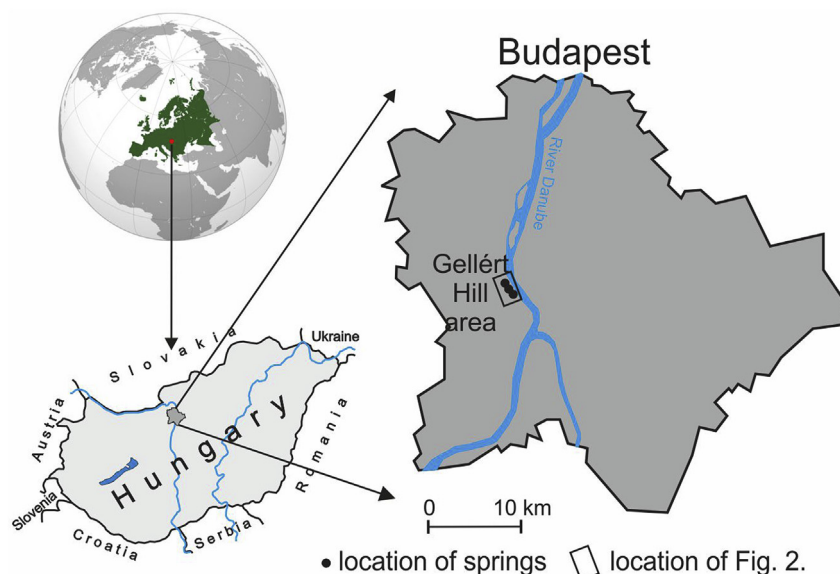


Fig. 1. The study area.

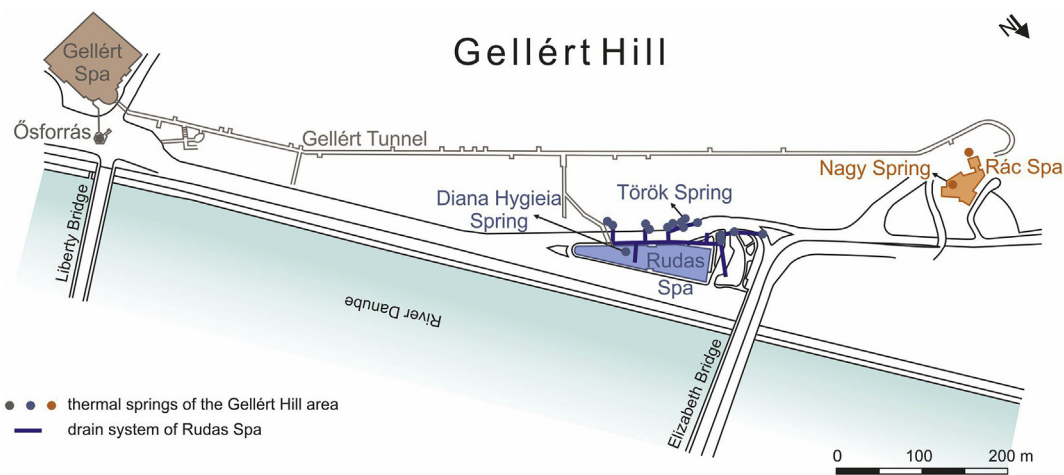


Fig. 2. Location of the spas and springs of Gellért Hill area, layout of Gellért Tunnel.

is a usual phenomenon in the springs of Gellért Hill, owing to the high  $\text{CO}_2$  and  $\text{HCO}_3^-$  content of the waters (Erőss, 2010; Erőss et al., 2012).

#### 2.4. Gellért Ósforrás

Ósforrás is a spring group, located in a huge hall, few meters under the road near Gellért Spa next to River Danube. The original spring discharges can be found at the bottom of the hall. There is a natural conduit at the back of the hall, it is a former spring cave, which is under water and BGP forms in it (Fig. 3d). The other part is artificial. The depth of the water is only a few meters. River Danube is close, so its effect is strong on the water level. The water surface is large, and also the air space above the water (Fig. 4d), which is highly ventilated.

#### 2.5. Gellért Tunnel

Gellért Tunnel was built between 1969 and 1978, after the spring waters got polluted. The original plan was to collect the thermal water inside the hill, before it discharges next to River Danube. The tunnel connects the Gellért, Rudas and Rác Spas. It is 1100 m long. A trapezoid

canal has been excavated into the concrete floor of the tunnel to canalize the overflow of thermal waters during high water level stages of River Danube. More information about the tunnel can be read in Kovács-Bodor et al. (2018).

### 3. Sampling and applied methods

#### 3.1. Survey of springs and related precipitates

There were two sampling campaigns of springs and related precipitates to survey all available springs, but it was not possible simultaneously. The study of temporal variations in the physicochemical parameters of the spring waters and the radioactivity was not a goal of this research. Based on previous measurements, when the flow conditions were more natural, the chemical composition of the spring waters is stable in time (Alföldi et al., 1968).

The first sampling was on the 6th December 2012 in Rác Nagy Spring, Rudas Diana Hygieia Spring and Gellért Ósforrás. The measured parameters, the applied methods or devices, the accuracy/detection limit of the measurements and the laboratories are summarized in

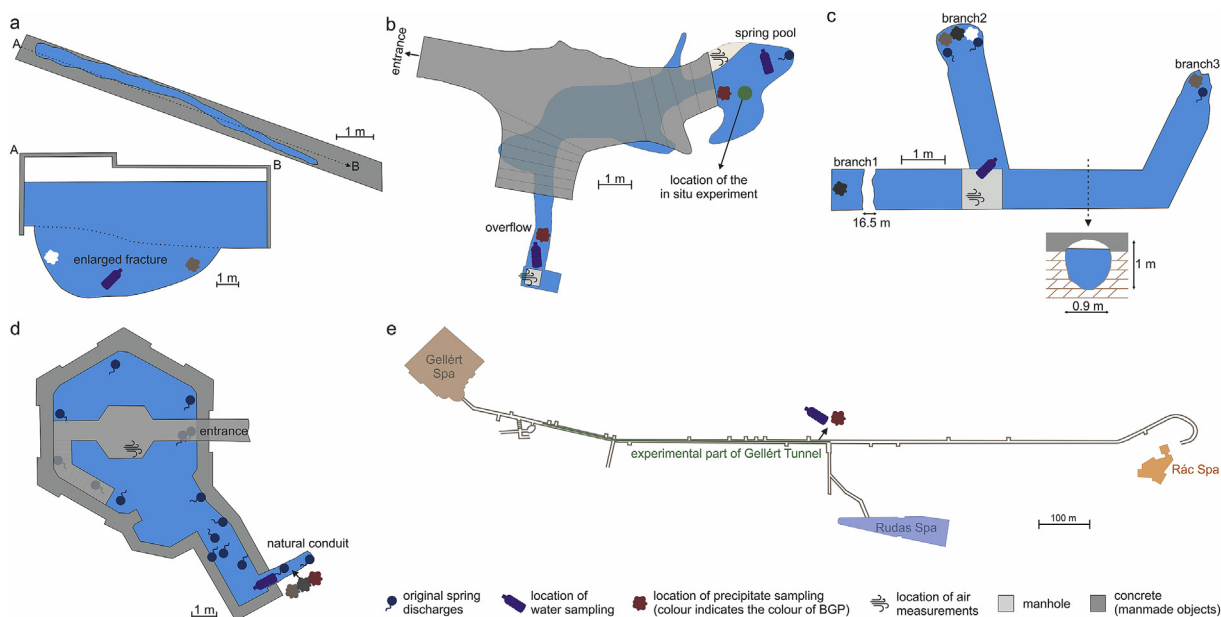


Fig. 3. The layout and sampling locations (modified after Alföldi et al., 1968) of a. Rác Nagy Spring, b. Rudas Török Spring, c. Rudas Diana Hygieia Spring, d. Gellért Ósforrás and e. Gellért Tunnel.

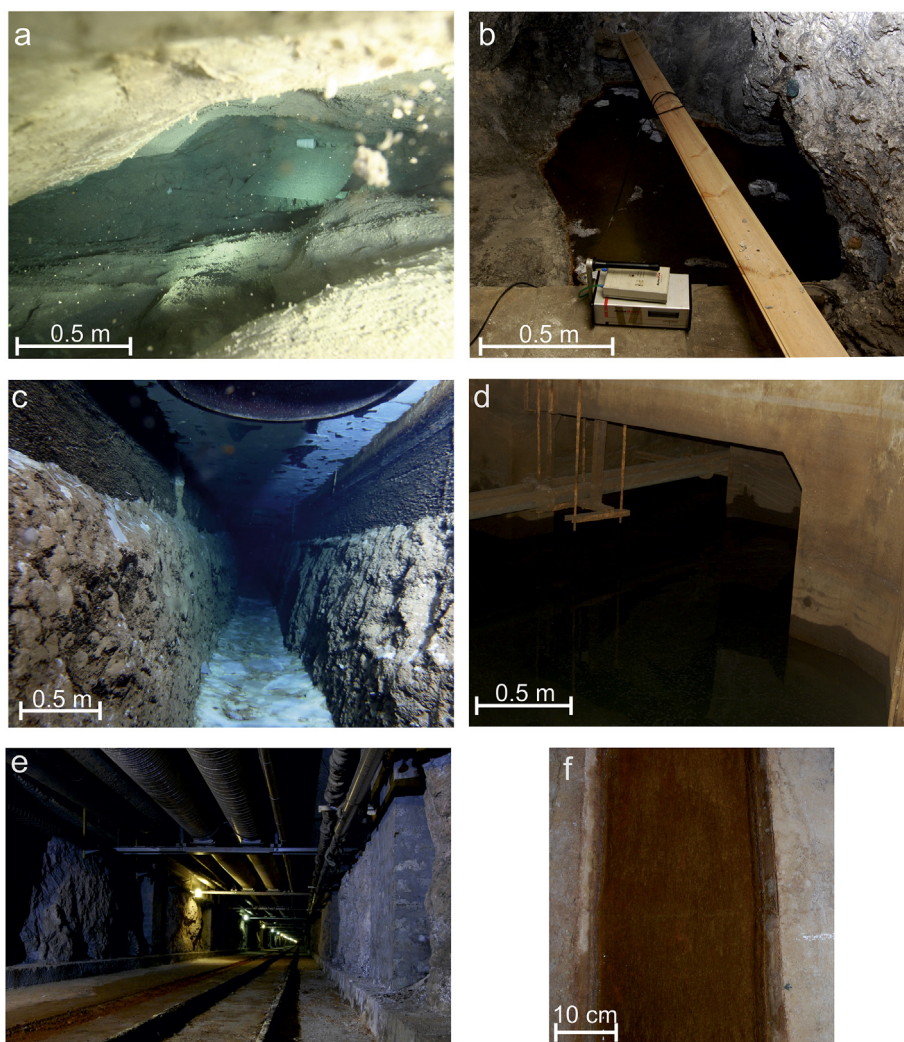


Fig. 4. a. The enlarged fissure of Rác Nagy Spring (photo: Sándor Kalinovits), b. The spring pool of Rudas Török Spring (photo: András Hegedűs), c. Branch 1 of Rudas Diana Hygieia Spring (photo: Dénes Szieberth), d. The hall of Gellért Ósforrás (photo: Katalin Csondor), e. Gellért Tunnel (photo: András Hegedűs), f. The canal in Gellért Tunnel (photo: András Hegedűs).

Table 1.

The second campaign was on the 26th March 2018 in Rudas Diana Hygieia Spring, Rudas Török Spring and Gellért Ósforrás. This time, Rác

Nagy Spring could not be sampled. The measured parameters, the applied methods or devices, the accuracy/detection limit of the measurements and the laboratories are summarized in Table 2. The

Table 1

Summary of the measured parameters, methods/devices, accuracies/detection limits and laboratories on 6th December 2012.

| Parameter  | Method                                      | Accuracy/detection limit   | Laboratory  |
|--|---|--|---|
| Temperature, specific electrical conductivity, pH, dissolved oxygen, redox potential | WTW Multi 350i                              | ± 0.3 °C for temperature<br>± 0.5% for specific electrical conductivity<br>± 0.004 for pH<br>± 0.5% for dissolved oxygen<br>± 1 mV for redox potential | On site   |
| HCO <sub>3</sub> <sup>-</sup>  | Alkalinity titration (ASTM 2320 B)          | ± 2%   | Department of Analytical Chemistry, ELTE <sup>a</sup> |
| Cl <sup>-</sup>  | Argentometric titrimetry (ASTM 4500-Cl-B)   | ± 2%   | Department of Analytical Chemistry, ELTE <sup>a</sup> |
| SO <sub>4</sub> <sup>2-</sup>  | Turbidimetric method (ASTM 4500-SO42-E)     | ± 5%   | Department of Analytical Chemistry, ELTE <sup>a</sup> |
| <sup>222</sup> Rn  | Liquid scintillation method TRICARB 1000 TR | min. 3 BqL <sup>-1</sup>   | Department of Atomic Physics, ELTE <sup>a</sup>       |
| Precipitates <sup>226</sup> Ra   | Gamma spectroscopy                          |  | Department of Atomic Physics, ELTE <sup>a</sup>       |

<sup>a</sup> Eötvös Loránd University.

**Table 2**

Summary of the measured parameters, methods/devices, accuracies/detection limits and laboratories on 26th March 2018 and of the in situ experiments.

| Parameter   | Method  | Accuracy/detection limit   | Laboratory   |
|---|---|--|--|
| Temperature, specific electrical conductivity, pH, dissolved oxygen, redox potential        | YSI Pro Plus  | ± 0.2 °C for temperature<br>± 0.5% for specific electrical conductivity<br>± 0.2 for pH<br>± 0.2 mgL <sup>-1</sup> for dissolved oxygen<br>± 20 mV for redox potential | On site  |
| Ca <sup>2+</sup>  | EDTA titrimetric method (ASTM 3500-Ca D)                  | ± 5 mgL <sup>-1</sup>  | Department of Physical and Applied Geology, ELTE <sup>a</sup>  |
| Mg <sup>2+</sup>  | EDTA titrimetric method (ASTM 3500-Mg E)                  | ± 2 mgL <sup>-1</sup>  | Department of Physical and Applied Geology, ELTE <sup>a</sup>  |
| Na <sup>+</sup> , K <sup>+</sup>  | Flame emission photometry (ASTM 3500-Na D, ASTM 3500-K D) | ± 2 mgL <sup>-1</sup> for Na <sup>+</sup><br>± 5 mgL <sup>-1</sup> for K <sup>+</sup>  | Department of Physical Geography, ELTE <sup>a</sup>  |
| HCO <sub>3</sub> <sup>-</sup>   | Alkalinity titration (ASTM 2320 B)                        | ± 12 mgL <sup>-1</sup>   | Department of Physical and Applied Geology, ELTE <sup>a</sup>  |
| Cl <sup>-</sup>   | Argentometric titrimetry (ASTM 4500-Cl-B)                 | ± 2 mgL <sup>-1</sup>  | Department of Physical and Applied Geology, ELTE <sup>a</sup>  |
| SO <sub>4</sub> <sup>2-</sup>   | Turbidimetric method (ASTM 4500-SO42-E)                   | ± 5 mgL <sup>-1</sup>  | Department of Physical and Applied Geology, ELTE <sup>a</sup>  |
| <sup>226</sup> Ra, <sup>234</sup> + <sup>238</sup> U  | Alpha spectrometry (Surbeck, 2000)                        | min. 10 mBqL <sup>-1</sup>   | Imre Müller and Heinz Surbeck Hydrogeology Laboratory of the Department of Physical and Applied Geology, ELTE <sup>a</sup> |
| <sup>222</sup> Rn   | Liquid scintillation method TRICARB 1000 TR               | min. 3 BqL <sup>-1</sup>   | Department of Atomic Physics, ELTE <sup>a</sup>  |
| Precipitates<br><sup>238</sup> U, <sup>226</sup> Ra, daughter elements of <sup>226</sup> Ra | Gamma spectroscopy  | peak area uncertainties ≤ 5% for most of the important peaks, except for <sup>234</sup> Th (high Compton background)   | Institute for Nuclear Research, Hungarian Academy of Sciences  |
| Air<br>Temperature, relative humidity, CO <sub>2</sub>                                      | Air Visual Pro  |  | On site  |
| <sup>222</sup> Rn   | AlphaGuard  | min. 2 Bqm <sup>-3</sup>   | On site  |

<sup>a</sup> Eötvös Loránd University.

sampling locations are indicated on the layout of springs and the tunnel (Fig. 3a–e).

At both occasions, the field parameters (temperature, specific electrical conductivity, pH, dissolved oxygen content and redox potential) were measured on site to know the basic physicochemical characteristics of the spring waters. For major ion analysis (Ca<sup>2+</sup>, Mg<sup>2+</sup>, Na<sup>+</sup>, K<sup>+</sup>, HCO<sub>3</sub><sup>-</sup>, Cl<sup>-</sup>, SO<sub>4</sub><sup>2-</sup>), water samples were collected in 1.5 L PET bottles with no head space and were kept cool until laboratory measurements (within 2 days). The concentration of ions was determined with the usual analytical laboratory techniques, following standard methods (Eaton et al., 2005). 10 ml water samples were injected into glass vials containing 10 ml Optifluor-O cocktail on site for the liquid scintillation of <sup>222</sup>Rn. The cap of the vial was additionally wrapped with parafilm and the AC was determined within 24 h. At the second occasion, water samples were collected into 0.25 L LDPE bottles for <sup>226</sup>Ra and <sup>234</sup>+<sup>238</sup>U AC analysis. The radionuclides were measured using Nucleonics discs, following the sample preparation and measurement described in Surbeck (2000). The samples were kept cool between the sampling and the measurements (within a week).

BGP samples were collected from the underwater walls of spring caves and branches with ceramic scalpels and syringes. As the BGP samples contained much water, they were centrifuged and after that dried at room temperature for 2 days before the gamma-spectrometry analysis in 2012. In 2018, the biofilm samples were lyophilized (UNICRYO MC2L-60) or centrifuged (Hettich Zentrifugen UNIVERSAL 32) and then lyophilized before the measurements.

The radioactivity of BGP samples at the 2012 sampling campaign was analysed by a GC1520-7500SL type HPGe detector.

Gamma-spectrometry measurements for the 2018 campaign have been carried out using a system based on a Canberra-Packard BE5030-7915-30ULB thin-windowed broad-energy HPGe detector (48% relative efficiency), equipped with DSA2000 multi-channel analyzer and Genie-2000 spectroscopy software v3.3 (incl. Gamma Analyses module and Interactive Peak Fit module). The dry samples have been packed into

either 50 mm or 90 mm diameter Petri dishes (depending on available sample sizes) and have been placed on a 1 mm thick plexiglass centering ring close to the detector cap for measurement. Efficiency calibrations have been performed using a point source set (provided by the Hungarian Metrological Institute) with efficiency transfer software ETNA (see e.g. Radu et al., 2009). The resulting efficiency curves have been validated using suitable reference materials, such as IAEA-385 (sediment) and IAEA-434 (phosphate/gypsum) CRMs packed into geometries similar to those of the samples.

The samples have been counted typically for 10–50 h, depending on ACs. Spectra have been evaluated for <sup>235</sup>U/<sup>226</sup>Ra through the 185.7–186.2 keV peaks. The interference of the 185.7 keV peak of <sup>235</sup>U with the 186.2 keV peak of <sup>226</sup>Ra has been corrected by calculation as well, with <sup>235</sup>U activity data coming either from the 143.8 keV peak (if evaluable) or by assuming natural <sup>235</sup>U/<sup>238</sup>U activity ratio. Activity concentrations (Bqkg<sup>-1</sup>) are expressed for dry mass.

At the second occasion the air parameters (<sup>222</sup>Rn content, relative humidity, CO<sub>2</sub> content, temperature) were measured first, before the inside air of spring cave or ducts were mixed with the outside air. As these springs are visited rarely, the water and the air have enough time to get into equilibrium. We measured this state of the air because of the degassing of <sup>222</sup>Rn.

### 3.2. Measurement of radioactivity in the frame of in situ experiments

The evolution of radioactivity of BGPs was determined based on the measurement of known-aged samples, formed during in situ experiments (Kovács-Bodor et al., 2017). Two in situ experiments were conducted in different flow conditions. Glass slides were put into the water in both experiments and BGPs were formed on these slides. One experiment was conducted in the spring pool of Török Spring, in a quasi-stagnant thermal water. The radioactivity of the formed BGP samples was measured after one year. The precipitation rate was slow in the quasi-stagnant water, one-year-old BGP had enough volume for the

**Table 3**  
Study sites and their codes.

| Study site                                | Code   |
|---|--------|
| Rác Nagy Spring                           | NAG    |
| Rudas Diana Hygieia Spring (branches 1–3) | DIA1-3 |
| Rudas Török Spring (spring pool)          | TOR/SP |
| Rudas Török Spring (overflow)             | TOR/OF |
| Gellért Ósforrás                          | OS     |
| Gellért Tunnel                            | GT     |

analysis. The other experiment was conducted in Gellért Tunnel. The ~37 °C warm water was pumped by invariable volume discharge ( $\sim 1.6 \cdot 10^{-4} \text{ m}^3 \text{ s}^{-1}$ ) from a thermal water well of Gellért Hill area into the canal. BGP was formed close to the beginning of the studied section of the canal (1 m far). The volume of BGP was enough for analysis after 12 weeks.

Water and BGP samples of the in situ experiments were prepared and measured with the same methods as the ones from the 2018 campaign (Table 2). Air parameters were not measured in Török Spring cave and in the tunnel at the time of the experiments.

## 4. Results and evaluation

### 4.1. Physicochemical parameters of spring waters

The measured and sampled springs are referred with their codes hereinafter (Table 3).

The data of field parameters, major ion concentrations and radionuclide activities of spring waters can be seen in Tables 4 and 5. The indicated results for TOR/SP are also valid for the in situ experiment conducted in the spring pool of Török Spring.

The field parameters were different for the studied spring waters, except pH, which was circumneutral (6.7–7.41) for all springs, including the water of GT. The temperature of the waters was between 29.1 and 37.6 °C in 2012 and between 23.1 and 35.3 °C in 2018. The temperature of the water of GT was 36.9 °C. Specific electrical conductivity was 1708–1808  $\mu\text{Scm}^{-1}$  in 2012 and 1740–1884  $\mu\text{Scm}^{-1}$  in 2018, 2007  $\mu\text{Scm}^{-1}$  in GT. OS had a little higher (by ~70–120  $\mu\text{Scm}^{-1}$ ) specific electrical conductivity than the other spring waters and also the water of GT (by ~250  $\mu\text{Scm}^{-1}$ ). Redox potential was negative (reducing; –250 mV) in NAG and positive (oxidizing; 95–166 mV in 2012, 21–152 mV in 2018) in the rest of the springs at both occasions. Dissolved oxygen content varied between 1.9 and 4.3  $\text{mgL}^{-1}$  in 2012 and 0.6–5.2  $\text{mgL}^{-1}$  in 2018, including the water of GT. The lowest content was measured in TOR/SP and TOR/OF.

The chemical composition of DIA, TOR/SP and TOR/OF are really similar to each other, while the anion concentrations are a little bit different for OS. There is less  $\text{HCO}_3^-$  and more  $\text{SO}_4^{2-}$  in the water of OS (Fig. 5).

At the first sampling campaign, the  $^{222}\text{Rn}$  AC was between 29 and 1102  $\text{BqL}^{-1}$  and between 24 and 1065  $\text{BqL}^{-1}$  at the second sampling campaign. At both occasions, OS had the minimum value and DIA had the maximum value. The  $^{222}\text{Rn}$  AC of the water used for the in situ experiment of Gellért Tunnel was  $214 \pm 13 \text{ BqL}^{-1}$ .  $^{226}\text{Ra}$  AC was

217–510  $\text{mBqL}^{-1}$ , including the water of GT, lowest in DIA, highest in TOR/SP.  $^{234+238}\text{U}$  AC was 62–117  $\text{mBqL}^{-1}$ , with minimum value in OS and maximum value in TOR/SP. The water of GT had lower  $^{234+238}\text{U}$  AC ( $26 \pm 5 \text{ mBqL}^{-1}$ ) than OS.

### 4.2. Radioactivity of precipitates

The sampled precipitates are referred with their codes hereinafter (Table 6).

The dried BGP mass was enough for radioactivity measurements only from Rác Nagy Spring and Gellért Ósforrás at the first sampling campaign. The results can be seen in Table 7.  $^{226}\text{Ra}$  AC of different coloured BGPs varied between 318 and 2226  $\text{Bqkg}^{-1}$ . RAC/WB had the lowest AC ( $318 \pm 11 \text{ Bqkg}^{-1}$ ), RAC/BB had higher AC ( $706 \pm 39 \text{ Bqkg}^{-1}$ ). The two BGP samples of Gellért Ósforrás (OS/B1 and OS/B2) had the same values within the error of analysis ( $2226 \pm 71$  and  $2144 \pm 72 \text{ Bqkg}^{-1}$ ).

In the 2018 sampling campaign, every sampled BGP was enough for analysis after lyophilization. The measured ACs of  $^{226}\text{Ra}$  and daughter isotopes of  $^{226}\text{Ra}$  can be seen in Table 8.  $^{226}\text{Ra}$  activities of precipitates were 150–187,000  $\text{Bqkg}^{-1}$ . The highest AC was in DIA3/BB ( $187,000 \pm 9000 \text{ Bqkg}^{-1}$ ). Much lower, but still high AC values were present in DIA1/DB ( $37,800 \pm 1900 \text{ Bqkg}^{-1}$ ) and DIA2/BP ( $36,900 \pm 3700 \text{ Bqkg}^{-1}$ ), compared to the other BGPs and precipitates. Lowest values were in the DIA2/WP ( $150 \pm 18 \text{ Bqkg}^{-1}$ ). TOR/SP/1 had  $220 \pm 10 \text{ Bqkg}^{-1}$   $^{226}\text{Ra}$  AC, much lower (by ~1800  $\text{Bqkg}^{-1}$ ) than the unknown aged BGP, sampled from the pool in 2018 (TOR/SP/RB). GT/12 had  $^{226}\text{Ra}$  AC of  $7950 \pm 440 \text{ Bqkg}^{-1}$ . The ACs of the daughter isotopes of  $^{226}\text{Ra}$  (the average of  $^{214}\text{Pb}$  and  $^{214}\text{Bi}$ ) changed between 72 and 30,600  $\text{Bqkg}^{-1}$ . The highest AC could be measured in DIA3/BB ( $30,600 \pm 300 \text{ Bqkg}^{-1}$ ), so in the case of  $^{226}\text{Ra}$ . The next highest value was almost one order of magnitude lower ( $3940 \pm 70 \text{ Bqkg}^{-1}$ , DIA2/BP). Lowest AC value was in DIA2/WP ( $72 \pm 2 \text{ Bqkg}^{-1}$ ).

Table 8 also contains the  $^{222}\text{Rn}$  emanation potential. By emanation potential we understand an empirical product of the emanation coefficient of radon atoms from the BGP grains to the pore gas/fluid and their subsequent exhalation probability to the open air/water bodies. The present data is insufficient for the differentiated estimation/calculation of the two terms, especially that of the exhalation rate, usually expressed in  $\text{Bqm}^{-2}\text{s}^{-1}$  (see Hassan et al., 2009). The  $^{222}\text{Rn}$  emanation potentials are higher than 64% for all BGPs. Its value is lower than 64% only for other precipitates than BGP (DIA2/WP  $52 \pm 6\%$ , TOR/OF/LP  $29 \pm 2\%$ ).

### 4.3. Air parameters

The data of measured air parameters can be seen in Table 9.

The temperature of the inside air of spring caves or canals were between 19.2 (OS) and 24.9 °C (TOR/SP). The relative humidity was around 100% everywhere (91–104%). The concentration of  $\text{CO}_2$  was the lowest in OS (670 ppm) and highest in TOR/SP (1768 ppm). The AC of  $^{222}\text{Rn}$  in the air was under the detection limit in DIA. Maximum values were in TOR/SP ( $7470 \pm 790 \text{ Bqm}^{-3}$ ). There is a significant drop in  $\text{CO}_2$  concentration and  $^{222}\text{Rn}$  AC between TOR/SP and TOR/OF

**Table 4**  
Data of field parameters, major anions and radionuclides of the 2012 sampling campaign.

| Study site code | Field parameters |   |      |                      |  | Major anions ( $\text{mgL}^{-1}$ ) |     |                    | Radionuclides                           |
|-----------------|------------------|---|------|----------------------|--|------------------------------------|-----|--------------------|---|
|                 | Temperature (°C) | Specific electrical conductivity ( $\mu\text{Scm}^{-1}$ ) | pH   | Redox potential (mV) | Dissolved oxygen content ( $\text{mgL}^{-1}$ ) | $\text{HCO}_3^-$                   | Cl- | $\text{SO}_4^{2-}$ | $^{222}\text{Rn}$ ( $\text{BqL}^{-1}$ ) |
| NAG             | 37.6             | 1735  | 6.70 | –250                 | 1.9  | 494                                | 114 | 506                | $160 \pm 8$                             |
| DIA             | 29.1             | 1708  | 7.07 | 166                  | 4.3  | 470                                | 122 | 506                | $1102 \pm 35$                           |
| OS              | 29.6             | 1808  | 7.05 | 95                   | 2.6  | 476                                | 137 | 506                | $29 \pm 3$                              |

**Table 5**  
Data of field parameters, major ions and radionuclides of the 2018 sampling campaign and the Gellért Tunnel in situ experiment.

| Study site code | Field parameters |  |      |                      | Major ions (mgL <sup>-1</sup> )               |                  |                  |                 |                |                               |                 | Radionuclides                 |   |   |  |
|-----------------|------------------|--|------|----------------------|---|------------------|------------------|-----------------|----------------|-------------------------------|-----------------|-------------------------------|---|---|--|
|                 | Temperature (°C) | Specific electrical conductivity (µScm <sup>-1</sup> ) | pH   | Redox potential (mV) | Dissolved oxygen content (mgL <sup>-1</sup> ) | Ca <sup>2+</sup> | Mg <sup>2+</sup> | Na <sup>+</sup> | K <sup>+</sup> | HCO <sub>3</sub> <sup>-</sup> | Cl <sup>-</sup> | SO <sub>4</sub> <sup>2-</sup> | <sup>226</sup> Ra (mBqL <sup>-1</sup> ) | <sup>234</sup> + <sup>238</sup> U (mBqL <sup>-1</sup> ) <sup>1)</sup> | <sup>222</sup> Rn (BqL <sup>-1</sup> ) |
| DIA             | 25.8             | 1.763  | 6.88 | 152                  | 2.4   | 171              | 58               | 139             | 18             | 524                           | 143             | 349                           | 217 ± 15                                | 87 ± 9  | 1065 ± 35                              |
| TOR/SP          | 35.3             | 1.742  | 6.70 | 88                   | 0.6   | 171              | 58               | 138             | 18             | 543                           | 127             | 345                           | 510 ± 23                                | 117 ± 11  | 579 ± 21                               |
| TOR/OF          | 33.0             | 1.74   | 7.00 | 21                   | 0.9   | 173              | 58               | 133             | 18             | 549                           | 129             | 350                           | 479 ± 22                                | 74 ± 9  | 519 ± 20                               |
| OS              | 23.1             | 1.884  | 7.41 | 84                   | 5.2   | 182              | 62               | 157             | 21             | 480                           | 167             | 430                           | 498 ± 22                                | 62 ± 8  | 24 ± 3                                 |
| GT              | 36.9             | 2.007  | 7.13 | n/a                  | 3.0   | 162              | 52               | 132             | 26             | 568                           | 140             | 299                           | 273 ± 17                                | 26 ± 5  | 214 ± 13                               |

(by ~800 ppm and 5000 Bqm<sup>-3</sup>, respectively).

### 5. Interpretation and discussion

As a result of the survey of the spring waters in Gellért Hill area, significant differences in the values of field parameters (temperature, specific electrical conductivity, pH, redox potential, dissolved oxygen content) and in the concentrations of major ions (Ca<sup>2+</sup>, Mg<sup>2+</sup>, Na<sup>+</sup>, K<sup>+</sup>, HCO<sub>3</sub><sup>-</sup>, Cl<sup>-</sup>, SO<sub>4</sub><sup>2-</sup>) were not found. In contrast, the ACs of radionuclides in the waters cover wide ranges, especially in case of <sup>222</sup>Rn (Table 4, Table 5).

These radionuclides can be used for the characterization of different waters with different origin because of their different geochemical behaviour (e.g. Eisenlohr and Surbeck, 1995; Hoehn, 1998) Their ACs should be in connection with temperature, specific electrical conductivity and redox potential. Eröss (2010) and Eröss et al. (2012) did not find linear connection between these parameters for spring and well waters of the Gellért Hill area. The same conclusion was driven from our measurements (Fig. 6a–i.)

The <sup>226</sup>Ra vs. <sup>222</sup>Rn activities in the water confirm the previous findings of Palotai et al. (2005), Eröss (2010) and Eröss et al. (2012), that the <sup>226</sup>Ra content of the water cannot be absolutely the source of the <sup>222</sup>Rn activity (Fig. 7a). While the highest <sup>226</sup>Ra AC was measured in Török Spring and Ósforrás, the lowest AC of <sup>222</sup>Rn was found in Gellért Ósforrás and the highest in Diana Hygieia Spring (Table 5, Fig. 7a).

We could find that the BGPs adsorb <sup>226</sup>Ra to varying degrees (Table 8). The most diverse BGPs could be collected from Diana Hygieia Spring, resulting in wide range of radioactivity of the precipitates. The different colour of BGPs can indicate different trace element concentrations, and maybe different contribution of chemical and biological processes in the BGPs' evolution. However, in the frame of this study it was not evaluated, we could see based on Dobosy et al. (2016) that in Ósforrás the enrichment factor (which compares the concentration of an element in the biogeochemical sample and in the water) has the greatest value for Fe (3698\*10<sup>8</sup>). The Fe(III) can be therefore responsible for the red colour based on the results from 57Fe Mössbauer spectroscopy. It was established that the iron-containing minerals are goethite (FeO(OH)), ferrihydrite (Fe<sub>2</sub>O<sub>3</sub>\*0.5H<sub>2</sub>O), hematite (Fe<sub>2</sub>O<sub>3</sub>) and siderite (FeCO<sub>3</sub>) in the BGPs (Kuzmann et al., 2014). The white precipitate of Diana Hygieia Spring (DIA2/WP) is most likely a chemical precipitate, so its radioactivity is closer to the value of the carbonate mud (360 ± 3 Bqkg<sup>-1</sup>) measured in Török Spring by Eröss (2010). The spring pool and the overflow of Török Spring have the same <sup>226</sup>Ra AC of water, but the radioactivity of BGPs are different. The <sup>226</sup>Ra AC of the laminated precipitate, collected in the overflow of Török Spring was lower than the “fresh” BGPs', because it is the alteration of BGP and carbonate. The BGPs in Ósforrás had similar radioactivity values (Table 8). Beside the <sup>226</sup>Ra content of the water other factors could affect the adsorption of BGPs, as there is no linear connection between <sup>226</sup>Ra AC of the water and the BGPs (Fig. 7b). A few of these factors could be the different adsorption capacity of BGPs (affected by the microbial diversity and the elemental composition of the BGPs, see the results of Diana Hygieia Spring, Anda et al., 2014), and the formation rate of them. The results of the in situ experiments reveal the different evolutionary rate of BGPs, influenced by the flow conditions, and it has an effect also on the radioactivity of the formed BGPs. The relatively high difference between the BGPs of the spring pool and overflow of Török Spring suggests also the role of flow conditions in radionuclide adsorption.

Most of the <sup>222</sup>Rn in the waters can be originated from the <sup>226</sup>Ra content of BGPs, revealed by the calculated high potential for radon emanation (64–97%) in their dried state and most likely in their wet state as well. There is also no clear connection between these parameters (Fig. 7c). Most BGPs have <sup>226</sup>Ra AC lower than 10,000 Bqkg<sup>-1</sup>, but the <sup>222</sup>Rn AC of waters vary between 24 and 1065 BqL<sup>-1</sup>.<sup>222</sup>Rn

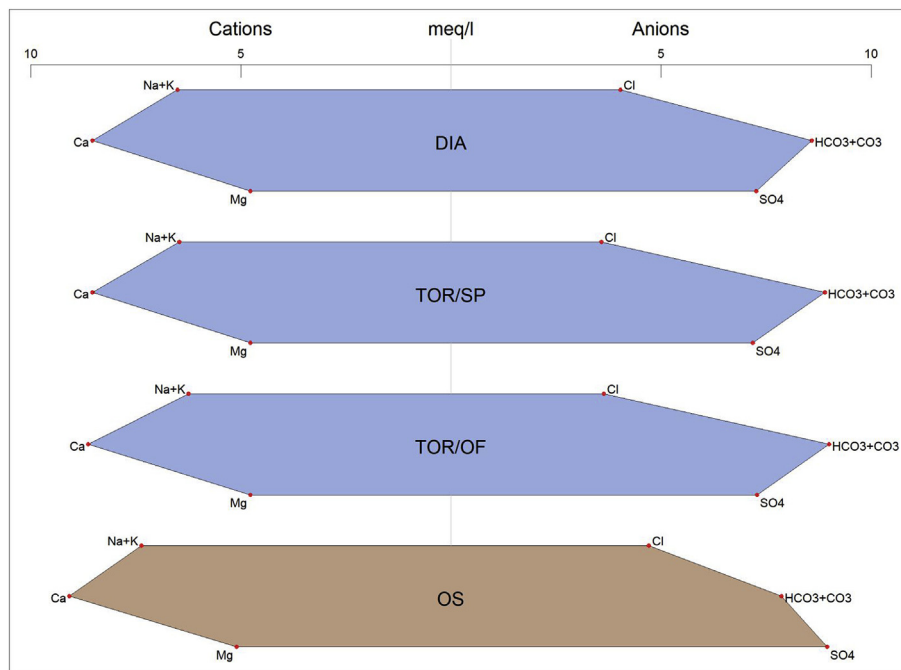


Fig. 5. Stiff diagrams of the studied spring water compositions.

Table 6  
Sampled precipitates and their abbreviations.

| Study site                              | BGP/precipitate     | Code      |
|---|---------------------|-----------|
| Rác Nagy Spring                         | White BGP           | NAG/WB    |
| Rác Nagy Spring                         | Brown BGP           | NAG/BB    |
| Gellért Ósforrás                        | BGP 1               | OS/B1     |
| Gellért Ósforrás                        | BGP 2               | OS/B2     |
| Rudas Diana Hygieia Spring (branches 1) | Dark BGP            | DIA1/DB   |
| Rudas Diana Hygieia Spring (branches 2) | Brown BGP           | DIA2/BB   |
| Rudas Diana Hygieia Spring (branches 2) | Black precipitate   | DIA2/BP   |
| Rudas Diana Hygieia Spring (branches 2) | White precipitate   | DIA2/WP   |
| Rudas Diana Hygieia Spring (branches 3) | Brown BGP           | DIA3/BB   |
| Rudas Török Spring (spring pool)        | Red BGP             | TOR/SP/RB |
| Rudas Török Spring (spring pool)        | 1-year-old BGP      | TOR/SP/1  |
| Rudas Török Spring (overflow)           | Red BGP             | TOR/OF/RB |
| Rudas Török Spring (overflow)           | Laminar precipitate | TOR/OF/LP |
| Gellért Ósforrás                        | Brown BGP           | OS/BB     |
| Gellért Ósforrás                        | Dark BGP            | OS/DB     |
| Gellért Ósforrás                        | Red BGP             | OS/RB     |
| Gellért Tunnel                          | 12-week-old BGP     | GT/12     |

Table 7  
Data of <sup>226</sup>Ra ACs of BGPs of the 2012 sampling campaign.

| BGP code | <sup>226</sup> Ra (Bqkg <sup>-1</sup> ) |
|----------|---|
| NAG/WB   | 318 ± 11                                |
| NAG/BB   | 706 ± 39                                |
| OS/B1    | 2226 ± 71                               |
| OS/B2    | 2144 ± 72                               |

degasses to the air from the water, which is affected by the area of water surface, volume of water and air space, ventilation of the springs, among others. The environment of springs is different (see chapters 2.1–2.4), which have a clear influence on the <sup>222</sup>Rn AC of water and air, causing a not linear connection between them (Fig. 7d). Diana Hygieia Spring had the highest <sup>222</sup>Rn AC, but the <sup>222</sup>Rn AC of the air was under the detection limit, though, it has a large water surface, but the spring is covered and has poor connection with the outside air. Probably the few mm thick, continuous calcite layer on the water surface is blocking

Table 8  
Data of <sup>226</sup>Ra and progeny ACs with <sup>222</sup>Rn emanation potential of BGPs of the 2018 sampling campaign and the Gellért Tunnel in situ experiment.

| BGP code  | Radionuclides (Bqkg <sup>-1</sup> ) |  | <sup>222</sup> Rn emanation potential (%) |
|-----------|-------------------------------------|--|---|
|           | <sup>226</sup> Ra                   | Daughter isotopes of <sup>226</sup> Ra |   |
| DIA1/DB   | 37,800 ± 1900                       | 1310 ± 20                              | 97 ± 5                                    |
| DIA2/BB   | 5400 ± 300                          | 1510 ± 20                              | 72 ± 4                                    |
| DIA2/BP   | 36,900 ± 3700                       | 3940 ± 70                              | 89 ± 9                                    |
| DIA2/WP   | 150 ± 18                            | 72 ± 2                                 | 52 ± 6                                    |
| DIA3/BB   | 187,000 ± 9000                      | 30,600 ± 300                           | 84 ± 4                                    |
| TOR/SP/RB | 2100 ± 140                          | 737 ± 10                               | 65 ± 4                                    |
| TOR/SP/1  | 220 ± 10                            | n/a                                    | n/a                                       |
| TOR/OF/RB | 9530 ± 550                          | 2640 ± 40                              | 72 ± 4                                    |
| TOR/OF/LP | 760 ± 45                            | 539 ± 6                                | 29 ± 2                                    |
| OS/BB     | 9370 ± 520                          | 3340 ± 40                              | 64 ± 4                                    |
| OS/DB     | 6840 ± 700                          | 2290 ± 40                              | 67 ± 7                                    |
| OS/RB     | 9650 ± 560                          | 1350 ± 20                              | 86 ± 5                                    |
| GT/12     | 7950 ± 440                          | 1050 ± 20                              | 87 ± 5                                    |

Table 9  
Data of air parameters measured during the 2018 sampling campaign.

| Study site code | Air parameters   |                       |                       |  |
|-----------------|------------------|-----------------------|-----------------------|--|
|                 | Temperature (°C) | Relative humidity (%) | CO <sub>2</sub> (ppm) | <sup>222</sup> Rn (Bqm <sup>-3</sup> ) |
| DIA             | 24.3             | 102                   | 1.338                 | under detection limit                  |
| TOR/SP          | 24.9             | 91                    | 1.768                 | 7470 ± 790                             |
| TOR/OF          | 22.0             | 104                   | 964                   | 2360 ± 415                             |
| OS              | 19.2             | 91                    | 670                   | 3930 ± 483                             |

degassing. The spring pool of Török Spring is partly covered by a concrete floor, and the cave is closed by a door, rarely visited, so here there is a higher chance for <sup>222</sup>Rn to get into equilibrium between the water and the air. In the overflow part of Török Spring, <sup>222</sup>Rn AC of air was significantly lower than near the spring pool (Table 9), because it is part of the drain system of Rudas Spa (Fig. 2), where it can easily escape

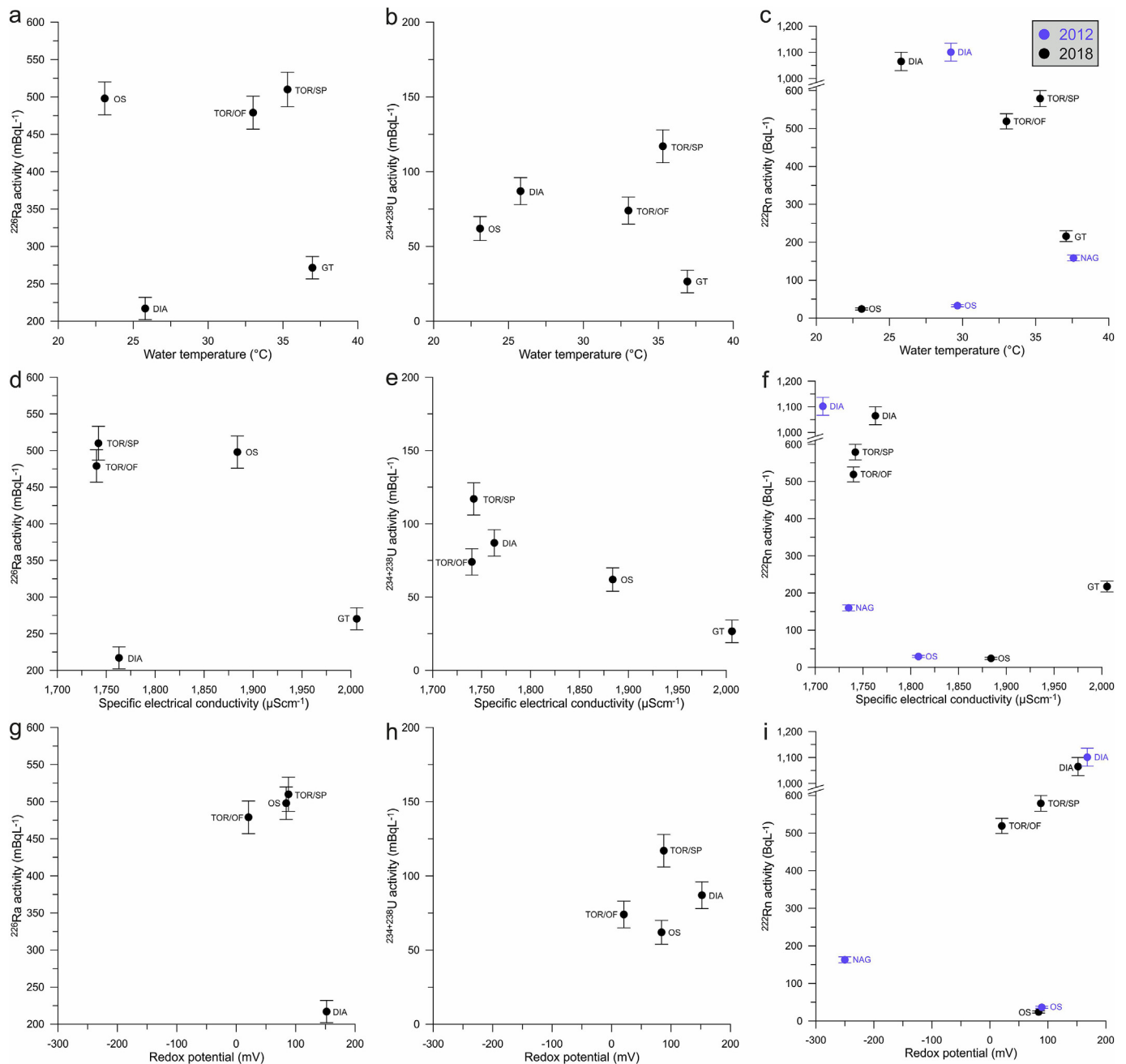


Fig. 6. Radionuclide ACs ( $^{226}\text{Ra}$ ,  $^{234} + ^{238}\text{U}$ ,  $^{222}\text{Rn}$ ) of the waters vs. a-c. water temperature, d-f. specific electrical conductivity and g-i. redox potential graphs.

to the outside air. Besides, flowing water helps degassing. Although Ósfórrás had the highest  $^{226}\text{Ra}$  AC, it also had the minimum  $^{222}\text{Rn}$  AC (Table 5). Here the water surface is large, so is the air space above it, which is ventilated.

### 6. Summary and conclusions

Radioactivity research have been performed for more than a hundred years in Buda Thermal Karst, but the  $^{222}\text{Rn}$  source of the waters was identified only about ten years ago. Biogeochemical precipitates adsorb  $^{226}\text{Ra}$  and produce  $^{222}\text{Rn}$ . This study resulted in more details about the radioactivity of waters and related precipitates in the Gellért Hill area of Buda Thermal Karst and could prove this previous hypothesis. There is no clear connection among the  $^{226}\text{Ra}$  activity concentration in the water, in the precipitates,  $^{222}\text{Rn}$  activity concentration in the waters and in the air connected to the springs. Based on our

measurements, some influencing factors could be detected. The  $^{226}\text{Ra}$  activity concentration of biogeochemical precipitates are affected by the adsorbing capacity of the precipitates (connected to microbial communities and elemental composition) and the rate of formation, besides  $^{226}\text{Ra}$  activity concentration of water. The rate of the evolution of biogeochemical precipitates are influenced by the flow conditions, which was proven by the conducted in situ experiments in quasi stagnant and flowing water.

The  $^{222}\text{Rn}$  activity of the water is also affected by degassing. Water surface, flow conditions, calcite layer on the water surface, volume of air space and the connection with the outside air have important role in degassing.

The simultaneous and detailed measurement of spring waters, related precipitates and air of the Gellért Hill area resulted in new conclusions of radioactivity of such environments. The exact role of microchemical characteristics (elemental composition), microbial

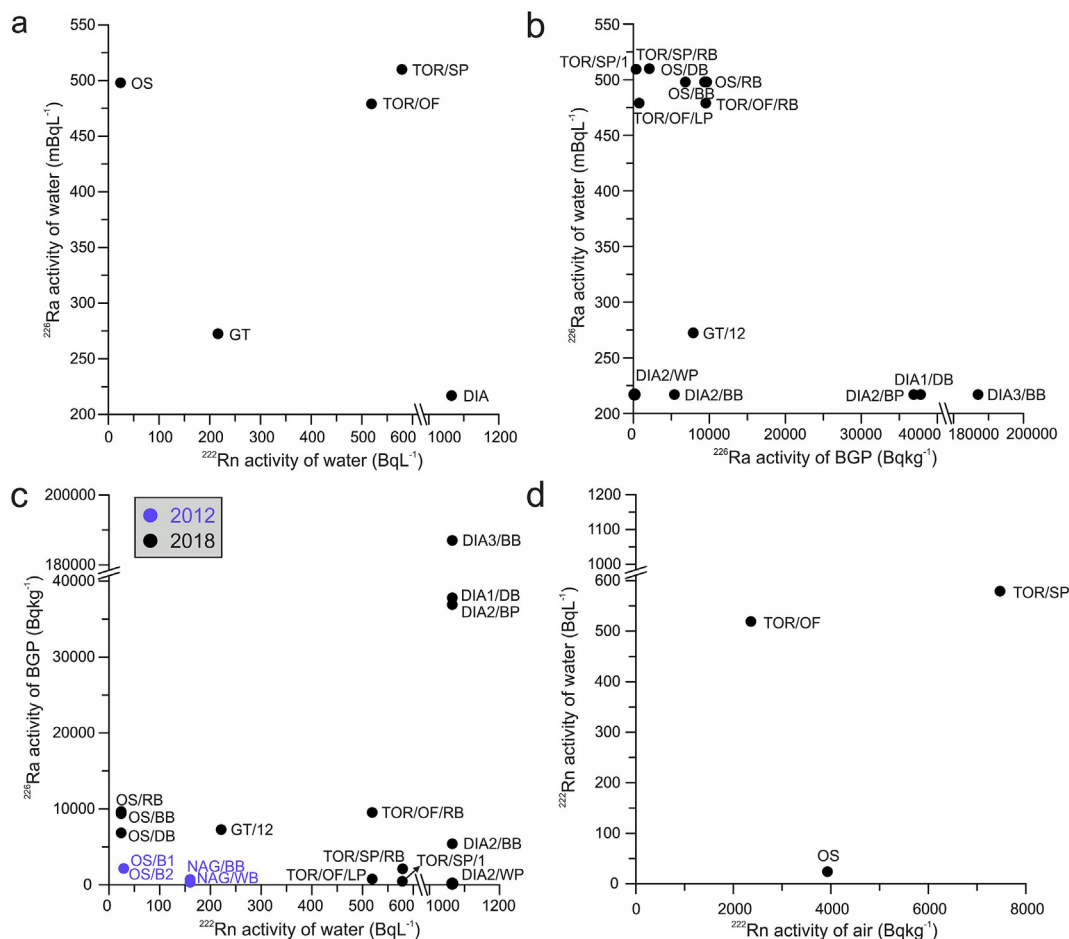


Fig. 7. The possible connections between the radioactivity of spring waters, BGPs and air.

diversity in the adsorption capacity of biogeochemical characteristics and the cause of different radionuclide content of chemically similar thermal waters needs further investigation. So as the activity of other radionuclides of the <sup>238</sup>U decay chain in the water and adsorbed in biogeochemical precipitates.

**Acknowledgement**

The research was supported by the National Research, Development and Innovation Office (NKFIH 101356) and the European Union and the State of Hungary, co-financed by the European Regional Development Fund in the project of GINOP-2.3.2.-15-2016-00009 ‘ICER’. The permission and help of Budapest Spa Plc. and the management of Gellért Spa are highly appreciated.

**References**

Alföldi, L., Béteky, L., Böcker, T., Horváth, J., Korim, K., Liebe, P., Rémi, R. (Eds.), 1968. Budapest Hévízei (Thermal Waters of Budapest) [in Hungarian]. VITUKI, Budapest.

Anda, D., Büki, G., Krett, G., Makk, J., Márialigeti, K., Eröss, A., Mádl-Szőnyi, J., Borsodi, A.K., 2014. Diversity and morphological structure of bacterial communities inhabiting the Diana-Hygieia thermal spring (Budapest, Hungary). *Acta Microbiol. Immunol. Hung.* 61 (3), 329–346.

Baradács, E., Hunyadi, I., Dezső, Z., Csige, I., Szerbin, P., 2001. <sup>226</sup>Ra in geothermal and bottled mineral waters of Hungary. *Radiat. Meas.* 34, 385–390.

Baradács, E., Dezső, Z., Hunyadi, I., Csige, I., Mócsy, I., Makfalvi, Z., Somay, P., 2002. Felszínalatti vizek maratontnyom-detektoros eljárással mért <sup>222</sup>Rn- és <sup>226</sup>Ra-tartalma (<sup>222</sup>Rn- and <sup>226</sup>Ra content of groundwaters, measured with etched track detection and bubbling methods). *Magy. Kem. Foly.* 108 (11), 492–500.

Borsodi, A.K., Knáb, M., Krett, G., Makk, J., Márialigeti, K., Eröss, A., Mádl-Szőnyi, J., 2012. Biofilm bacterial communities inhabiting the cave walls of the Buda thermal karst system, Hungary. *Geomicrobiol. J.* 29 (7), 611–627. <https://doi.org/10.1080/01490451.2011.602801>.

Dobosy, P., Sávoly, Z., Óvári, M., Mádl-Szőnyi, J., Záray, Gy., 2016. Microchemical characterization of biogeochemical samples collected from the Buda thermal karst system, Hungary. *Microchem. J.* 124, 116–120. <https://doi.org/10.1016/j.micro.2015.08.004>.

Eaton, A.D., Clesceri, L.S., Rice, E.W., Greenberg, A.E., Franson, M.A.H. (Eds.), 2005. *Standard Methods for the Examination of Water and Wastewater*, twenty-first ed. American Public Health Association, Washington.

Eisenlohr, L., Surbeck, H., 1995. Radon as a natural tracer to study transport processes in a karst system. An example in the Swiss Jura. *C.R. Acad. Sci. Paris, Sciences de la terre et des planets* 321 (2a), 761–767.

Enyedi, N.T., Anda, D., Borsodi, A.K., Szabó, A., Pál, S.E., Óvári, M., Márialigeti, K., Kovács-Bodor, P., Mádl-Szőnyi, J., Makk, J. Radioactive environment adapted bacterial communities constituting the biofilms of hydrothermal spring caves (Budapest, Hungary). accepted to *J. Environ. Radioact.*

Erhardt, I., Ótvös, V., Eröss, A., Czauner, B., Simon, Sz., Mádl-Szőnyi, J., 2017. Hydraulic evaluation of the hypogenic karst area in Budapest (Hungary). *Hydrogeol. J.* 25 (6), 1871–1891. <https://doi.org/10.1007/s1004-0-017-1591-3>.

Eröss, A., 2010. *Characterization of Fluids and Evaluation of Their Effects on Karst Development at the Rózsadomb and Gellért Hill, Buda Thermal Karst, Hungary*. Dissertation, Eötvös Loránd University.

Eröss, A., Mádl-Szőnyi, J., Surbeck, H., Horváth, Á., Goldscheider, N., Csoma, É.A., 2012. Radionuclides as natural tracers for the characterization of fluids in regional discharge areas, Buda Thermal Karst, Hungary. *J. Hydrol.* 426–427, 124–137. <https://doi.org/10.1016/j.jhydrol.2012.01.031>.

Hassan, N.M., Hosoda, M., Ishikawa, T., Sorimachi, A., Sahoo, S.K., Tokonami, S., Fukushi, M., 2009. Radon migration process and its influence factors; review. *Jpn. J. Health Phys.* 44, 218–231. <https://doi.org/10.5453/jhps.44.218>.

Hoehn, E., 1998. Radionuclides in groundwaters: contaminants and tracers. In: Herbert, M., Kovar, K. (Eds.), *Groundwater Quality: Remediation and Protection*. IAHS Publ. No. 250, pp. 3–9.

Kasztovszky, Zs, Kuczai, R., Szerbin, P., 1996. On the natural radioactivity of waters in Hungary. *Cent. Eur. J. Occup. Environ. Med* 2 (4), 335–347.

Kovács-Bodor, P., Anda, D., Burkus, V., Óvári, M., Horváth, Á., Kuzmann, E., Homonnay, Z., Futó, I., Makk, J., Borsodi, A.K., Mindszenty, A., Mádl-Szőnyi, J., 2017. Evolution of bacterial biofilms and chemical precipitates in thermal springs depending on flow kinetics (Buda Thermal Karst, Hungary). In: Posavec, K., Marković, T. (Eds.), 44th Annual Congress of the International Association of Hydrogeologists (IAH) “Groundwater Heritage and Sustainability”, Book of Abstracts, pp. 317.

- Kovács-Bodor, P., Anda, D., Jurecska, L., Óvári, M., Horváth, Á., Makk, J., Post, V., Müller, I., Mádl-Szőnyi, J., 2018. Integration of in situ experiments and numerical simulations to reveal the physicochemical circumstances of organic and inorganic precipitation at a thermal spring. *Aquat. Geochem.* 24, 231–255. <https://doi.org/10.1007/s10498-018-9341-2>.
- Kuzmann, E., Hommonay, Z., Kovács, K., Zsabka, P., Erőss, A., Mádl-Szőnyi, J., 2014. Mössbauer study of biofilms formed at spring caves of Buda Karst, Hungary. *Hyperfine Interact.* 226, 571–577. <https://doi.org/10.1007/s10751-013-0932-4>.
- Mádl-Szőnyi, J., Erőss, A., Tóth, Á., 2017. Fluid flow systems and hypogene karst of the Transdanubian Range, Hungary—with special emphasis on Buda Thermal Karst. In: Klimchouk, A., Palmer, A., De Waele, J., Auler, A., Audra, P. (Eds.), *Hypogene Karst Regions and Caves of the World*. Springer, Cham. <https://doi.org/10.1007/978-3-319-53348-3>.
- Makk, J., Tóth, E.M., Anda, D., Pál, S., Schumann, P., Kovács, A.L., Mádl-Szőnyi, J., Márialigeti, K., Borsodi, A.K., 2016. *Deinococcus budaensis* sp.nov., a mesophilic species isolated from a biofilm sample of a hydrothermal spring cave. *Int. J. Syst. Evol. Microbiol.* 66, 5345–5351. <https://doi.org/10.1099/ijsem.0.001519>.
- Páll-Somogyi, K., 2010. A Duna hatásának vizsgálata a Gellért-hegy környezetének felszín alatti vizeire (The study of the effect of River Danube on the groundwater of Gellért Hill area) [in Hungarian]. *Hidrol. Tájékoztató* 50 (1), 23–24.
- Palotai, M., Mádl-Szőnyi, J., Horváth, Á., 2005. A Budapest Gellért- és a József-hegy felszín alatti vizeiben mért radon- és rádiumtartalom lehetséges forrásai (Potential radon and radium sources for subsurface water of Gellért and József Hills, Budapest, Hungary) [in Hungarian]. *Ált. Föld. Szemle* 29, 25–40.
- Radu, D., Stanga, D., Sima, O., 2009. ETNA software used for efficiency transfer from a point source to other geometries. *Appl. Radiat. Isot.* 67, 1686–1690. <https://doi.org/10.1016/j.apradiso.2009.02.088>.
- Surbeck, H., 2000. Alpha spectrometry sample preparation using selectively adsorbing thin films. *Appl. Radiat. Isot.* 53, 97–100. [https://doi.org/10.1016/S0969-8043\(00\)00119-6](https://doi.org/10.1016/S0969-8043(00)00119-6).
- Weszelszky, Gy., 1912. A budapesti hévizek radioaktivitásáról és eredetéről (Radioactivity of the thermal waters of Budapest) [in Hungarian]. *Mat. term.tud. Ért.* 30, 340–381.